An Introduction to Synthetic Aperture Radar: a High-Resolution Alternative to Optical Imaging

Mark T. Crockett

Abstract—**Optical methods for data collection on spacecraft and aircraft have been in use for many decades. In the late 1970s, radar became a standard component in space-borne remote sensing systems. Radar imagers are especially useful for space-borne and airborne applications because in the microwave frequency band, they operate independent of atmospheric conditions like clouds, rain, snow, fog, daylight, etc. unlike optical imagers. Synthetic Aperture Radar (SAR) systems are radar imagers that exploit the collection of many independent samples of targets in a particular scene to produce intrinsically high-resolution images and have several key advantages over airborne optical imagers.**

I. Introduction

Synthetic Aperture Radar (SAR) systems are sophisticated imaging systems that emit electromagnetic (EM) radiation at microwave frequencies (300 MHz to 300 GHz). As opposed to optical imaging systems, which measure the visible spectrum return of solar EM radiation in a particular scene, SAR systems illuminate the scene of interest with their own transmit signal. Fig. I shows an example of a high-resolution SAR image. Applications of SAR include intelligence, surveillance, and reconnaissance, interferometry, foliage penetration, moving target indication, and environmental monitoring. SAR is often preferred over optical imagers for these applications because its performance is independent of available daylight and visibility.

From a high-level perspective, SAR systems emit microwaves at a scene and measure the voltage returned from a scene of targets. From these voltages, the radar cross-section (RCS) is found, which is a measure of how "large" a target appears in a radar image. High values of RCS show up as bright targets, whereas targets with low RCS are dim. Targets with rough surfaces tend to scatter EM radiation back towards the radar, so man-made targets like buildings, vehicles, and roads have a high RCS. Since the ground is relatively flat, it scatters EM radiation away from the radar and its RCS is low. Because RCS is a measure of how much of a transmitted signal is scattered back towards the radar, it is also called backscatter, which will be used synonymously with RCS in this paper.

Fig. 1. Ku-band SAR image of the Pentagon in Washington, D.C. (Courtesy Sandia National Laboratories).

This paper takes a high-level approach to discussing SAR systems and their operation, geometry, and image processing. Section II outlines the physical geometry that enables SAR systems to be such versatile radar imagers. In Section III, the signal properties of SAR are discussed, which is followed by an explanation of SAR signal and image processing in Section IV. Finally, Section V makes a practical comparison between optical imagers and SAR systems.

II. SAR Geometry

This section discusses the basic concept of SAR imaging, including its physical geometry and modes of operation. Three types of SAR collection are typically used, including stripmap, spotlight, and scanSAR modes. In stripmap mode, the antenna boresight is in a fixed position, and may be orthogonal to the flight path or squinted slightly forward or backward. Spotlight SAR utilizes a gimballed antenna in order to maintain dwell time on a chosen target for as long as possible. Finally, scanSAR mode scans the antenna pattern outwards from the radar platform during each pulse to increase the width of the imaging swath. This paper deals exclusively with stripmap SAR.
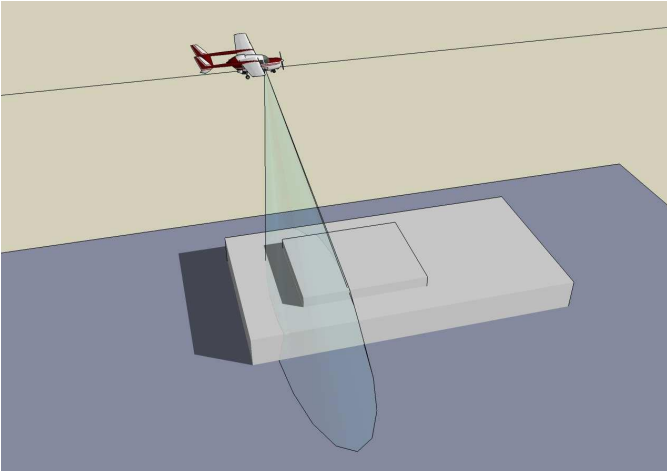
Fig. 2. Stripmap SAR imaging mode. Azimuth is described by the direction of the aircraft flight path and range is in the direction pointed by the antenna, which is orthogonal to the azimuth direction (Courtesy Evan Zaugg, Brigham Young University).

SAR has been in use for radar imaging for more than 50 years, and its capabilities are consistently being expanded. However, the fundamental concepts that allow SAR to work so well have been in use since its conception in the late 1950s. The primary theory that is exploited is that SAR antenna geometry facilitates the collection of many independent samples for an individual target, thus enabling fine spatial resolution. Fig. 2 shows the antenna geometry for a mobile SAR platform operating in stripmap mode. As the antenna aperture moves along the flight path, a signal is transmitted at a rate equal to the pulse repetition frequency (PRF). The lower bound of the PRF is determined by the Doppler bandwidth of the radar, which is the range of Doppler frequencies observed by the radar during the collection. Conversely, the PRF must be low enough that returns from the far edge of the scene for one pulse are measured before the detecting signal returns from the near edge of the scene of the next pulse. The backscatter return of each of these pulses is coherently summed on a pixel-by-pixel basis to attain the fine azimuth resolution desired in radar imagery. Real aperture radar imaging requires an antenna that is long in the azimuth direction to produce a narrow beamwidth (and hence fine resolution), which gives the azimuth resolution Δy_R [1],

$$\Delta y_R = 2R \sin\left(\frac{\beta_y}{2}\right) \approx R\beta_y = \frac{\lambda R}{l_y} \qquad (1)$$

where R is the slant range from the radar platform to the target, β_y is the 3dB azimuth beamwidth, λ is the wavelength of the transmitted pulse, and l_y is the length of the antenna aperture in the azimuth direction. The first approximation is an application of the small

angle approximation, where $\sin\left(\frac{\beta_y}{2}\right) \approx \frac{\beta_y}{2}$, and the second uses the approximation of the beamwidth from the physical dimensions of the antenna ($\beta \approx \frac{\lambda}{l_y}$). In contrast, SAR azimuth resolution (Δy_S) is independent of range [1], and improves with decreasing antenna size (or increasing antenna beamwidth)

$$\Delta y_S = \frac{\lambda}{4\sin\frac{\beta_y}{2}} \approx \frac{\lambda}{2\beta_y} \approx \frac{l_y}{2}. \qquad (2)$$

Likewise, the range resolution of SAR is also independent of the range to the target [1]

$$\Delta x_{LFM} = \frac{c_0}{2BW} \qquad (3)$$

where c_0 is the speed of light and BW is the radar bandwidth, which is fixed for any particular SAR collection. Therefore, regardless of the range of the radar platform to the target, SAR image resolution is fixed. SAR antenna geometry allows for very small and lightweight radar platforms and very fine resolution, which make it ideal for airborne radar imaging systems.

III. SIGNAL PROPERTIES

Traditional SAR systems consist of either two co-located antenna apertures (one for transmission and one for reception) or a single aperture that alternates between both transmit and receive modes. The radar equation for a point target gives the received power (P_r) for a single target for a particular pulse, and is given by

$$P_r = \frac{P_t G^2 \lambda^2}{(4\pi)^3 R^4} \sigma, \qquad (4)$$

where P_t is the transmitted power, G is the antenna gain, and σ is the radar cross-section [2]. The radar equation is paramount to determining backscatter values for each pixel in an image grid and in SAR image processing.

The earliest SAR systems employed a transmitted radar signal that consists of a single frequency and a very short pulse duration in order to attain fine image resolution. These are called interrupted continuous wave (ICW) SARs and have a duty cycle of less than 100%. This short pulse duration results in extreme instantaneous power requirements for a reasonable signal-to-noise ratio (SNR) (ratio of returned signal energy to noise energy) and is somewhat impractical to implement in hardware. Today, the most common SAR systems utilize a linear frequency modulated (LFM) signal. An LFM signal is a "chirped" signal in that the its frequency changes linearly throughout the duration of the pulse. The range of frequencies of an LFM signal is what determines the signal bandwidth. LFM signals also have longer pulse
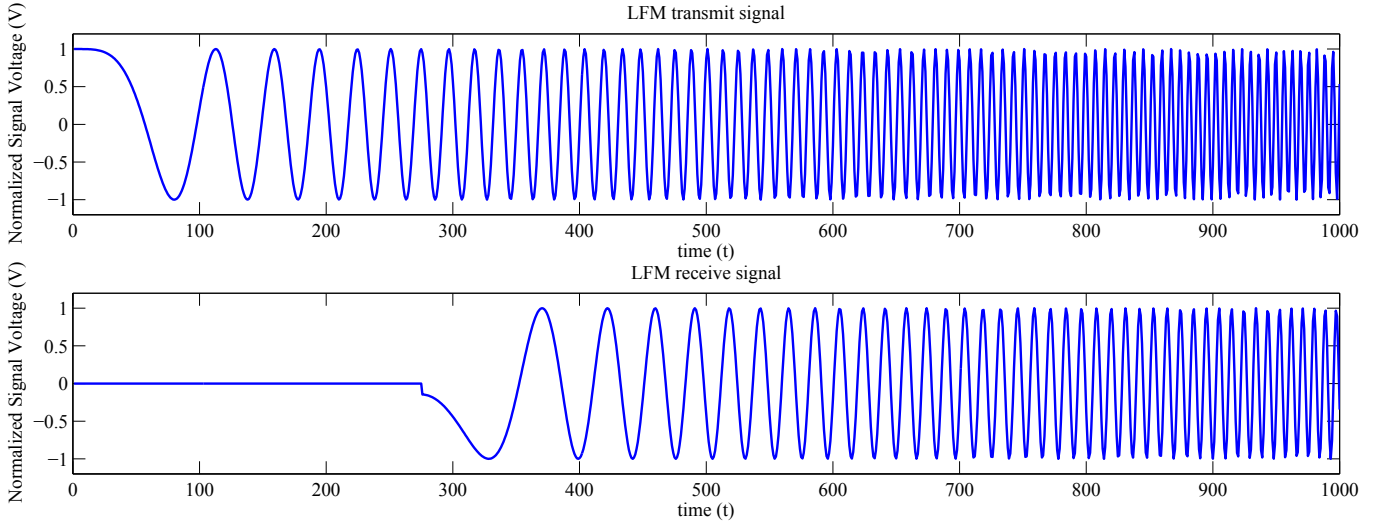
Fig. 3. LFM transmit and receive signals.

lengths than those of ICW systems, so they carry more energy per pulse than ICW signals, thus decreasing the instantaneous power requirement of LFM SAR systems.
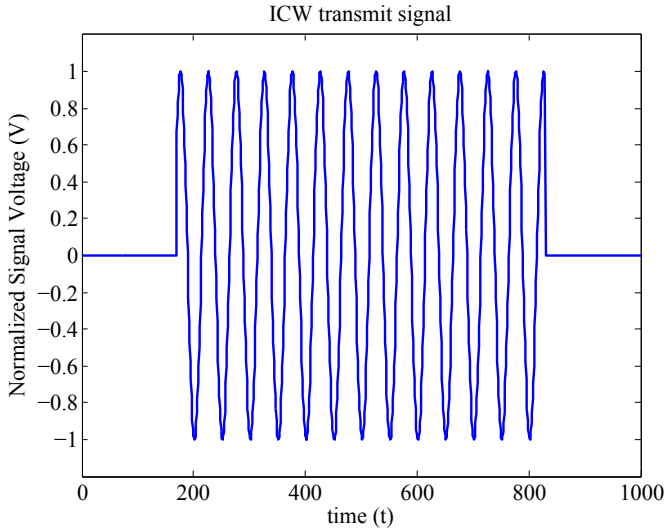

Fig. 4. A rectangular-windowed ICW transmit pulse.

$$\Delta x_{ICW} = \frac{c_0 T}{2} \qquad (5)$$

Note from Eq. (5) that range resolution for ICW systems is directly proportional to pulse duration T [3]. This means that impractically short pulses are needed to attain the equivalent range resolution of LFM systems, which is given in Eq. (3), and can be improved by increasing the range of frequencies over which the LFM signal is swept.

A very narrow pulse width creates a problem when seeking reasonable SNR. Since SNR is generally a key measure of performance of a radar system, high SNR is desirable. Total energy of the transmit signal must be increased in order to achieve this, which means increasing the instantaneous power of each pulse. It is here that ICW systems become impractical, since narrow pulse widths are required for fine range resolution, but long pulses are required for high energy and performance. LFM SAR systems overcome these barriers because the total transmit energy can be increased by lengthening the pulse duration without sacrificing range resolution.

A zero-phase LFM transmit signal can be expressed as

$$s_t(t) = A(t) \exp\left(\jmath\left(2\pi f_0 t + \pi k_r t^2\right)\right) \qquad (6)$$

where $A(t)$ is the signal amplitude at time t, f_0 is the frequency at the beginning of the chirp, and k_r is the chirp rate [4]. A transmitted signal propagates through the atmosphere (which is approximated as free space) and is scattered throughout the target scene. Generally, most of the transmit energy is scattered away from the radar, so a very small amount of energy is received. The received signal for an individual point target can be expressed as

$$s_r(t) = A'(t) \exp\left(\jmath\left(2\pi f_0 (t - \tau) + \pi k_r (t - \tau)^2\right)\right) \quad (7)$$

where $A'(t)$ is an attenuated version of $A(t)$ and τ is the two-way time of flight from the radar to the target at range R, and is given by

$$\tau = \frac{2R}{c_0}. \qquad (8)$$

For simplicity in processing, the receive signal is mixed down to baseband, meaning that the carrier frequency of

the signal is near zero. This mixed down signal is

$$s_{rmd}(t) = A'(t) \exp(\jmath(2\pi(f_0 - f_{md})t \\ - 2\pi f_0 \tau + \pi k_r(t-\tau)^2)) \qquad (9)$$

IV. IMAGE PROCESSING

In order to be useful as a high-resolution imagery, SAR data must be processed in steps. These steps include range compression, range cell migration correction, and azimuth compression. This section gives a brief overview of this process as well as an algorithm that processes the range-compressed data.

Since the return SAR signal is an attenuated, time-shifted copy of the transmit signal, a reference signal is defined to be equal to the transmit signal. The idea behind range compression is to correlate the receive signal with the reference signal in order to pull out the range information of the target. This is recognized as a matched filter and is implemented simply by applying the fast Fourier transform (FFT) to each signal, performing a complex multiply of the two, and performing an inverse FFT on the product. The result of such an procedure is shown in Fig. 5.
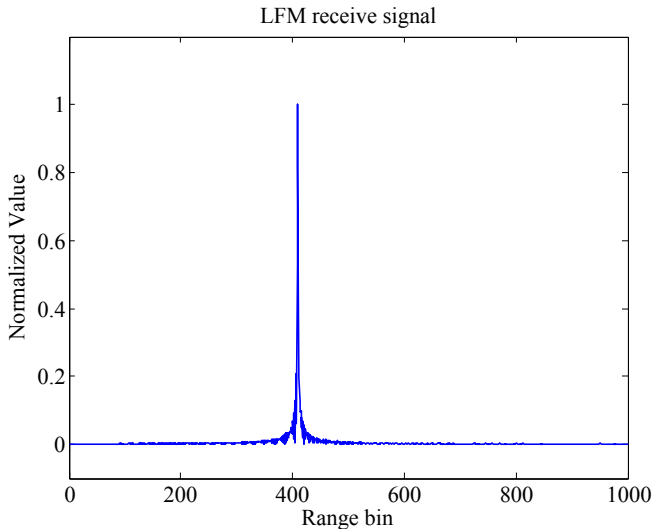

Fig. 5.   LFM range-compressed data.

Since most SARs use an antenna with a wide azimuth beamwidth, targets are imaged for a period of time long enough that their signatures are detected in multiple range bins (range resolution cells) through the length of the synthetic aperture. This effect can be seen in the second image of Fig. 6. To alleviate this issue, the trajectories are shifted so that for a single target, they all fall in the same range bin for the entire synthetic aperture. Finally, azimuth compression is performed on that data with another matched filter applied in the azimuth direction for each range bin [4]. The result is a focused image similar to the fourth image in Fig. 6.

Many SAR image formation algorithms have been developed for processing range-compressed data and are currently in use, including the range Doppler, omega-k, and backprojection algorithms (BPA)[1]. Backprojection is the most accurate and robust of these, but it is the most computationally expensive. However, recent technologies with massively-parallelized graphics processing have made the computation expense of backprojection very manageable. Fig. 7 and Fig. 8 are examples of range-compressed SAR data $S_R(r[n])$, processed using the backprojection algorithm, which, for a pixel at (x_0, y_0, z_0), may be expressed by

$$A(x_0, y_0, z_0) = \sum_n S_R(r[n]) e^{\jmath \Phi_e(r[n])}, \qquad (10)$$

where $A(x_0, y_0, z_0)$ is the complex power in that pixel, $r[n]$ is the range from the pixel location to the antenna phase center for pulse n, and $\Phi_e(r[n])$ is the complex conjugate of the expected phase of $r[n]$ [4].

V. COMPARISON

The primary differences in SAR and optical images are caused by the properties of the targets being imaged. These include dielectric properties, which describe how much a material insulates from an electric charge, and surface roughness, which determines the direction of EM scattering. Two primary reasons why targets appear differently between SAR and optical images are that dielectrics reflect radiation in a manner dependent on the frequency of the radiation, and surface roughness on the order of centimeters cause significant scattering (higher backscatter) in SAR imagery, whereas this occurs at the micrometer level in optical imagery.

Both SAR and optical imagers have benefits and shortcomings. Optical imagers can produce much finer resolution images than SAR and are generally low power devices. They can also produce true color images, which may sometimes be beneficial in airborne surveillance. SAR, on the other hand, is unaffected by clouds, fog, or other impairments to visibility. Also, since it provides its own target illumination, it works just as effectively at night as during the daytime. Furthermore, SAR signals

---

[1]In order to form a focused image, BPA assumes knowledge of the physical position of the antenna during each transmit pulse as a reference in determining the location of each target. Many SAR systems employ a Global Positioning System coupled with an inertial measurement unit (IMU) to obtain a precise estimate of this position. This measurement of the antenna location allows the precise target location to be determined.
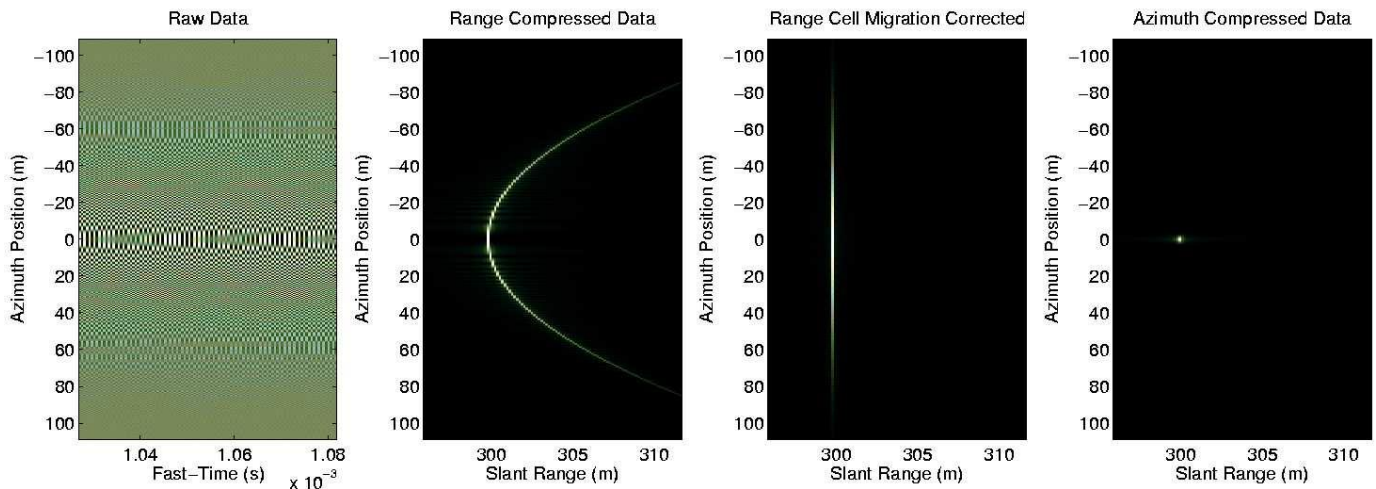
Fig. 6. Simulated SAR data for a point target. From left to right the SAR data is shown as raw data, and after range compression, range cell migration correction, and azimuth compression (Courtesy Evan Zaugg, Brigham Young University).

Fig. 7. SAR image of Spanish Fork, UT compared side-by-side with a corresponding Google Earth image (Courtesy Artemis Inc. and Google Inc.).

can penetrate foliage and dry ground for useful reconnaissance purposes.

Fig. 7 and Fig. 8 make side-by-side comparisons of a SAR image and an optical image for two identical scenes. Fig. 7 is an image of a residential area. Note that although the asphalt is optically bright, it shows up black in the SAR image, and vice versa for the shingles on the roofs of homes. In general, it can be seen that man-made structures are easily detectable in SAR images. Notice in Fig. 8 that while terrain is fairly easily distinguishable in the optical image, it is not so for the SAR image. Also, much of the vegetation is bright in the SAR image

because it scatters a significant amount of radiation back to the radar antenna.

VI. CONCLUSION

SAR systems utilize simple geometry, precise GPS location estimation, and accurate image processing algorithms to produce high-resolution images. They can be lightweight, low power, highly scalable systems and used in a variety of applications, both military and civilian. Both optical and SAR imagery are used in these applications. Each have their advantages and drawbacks,
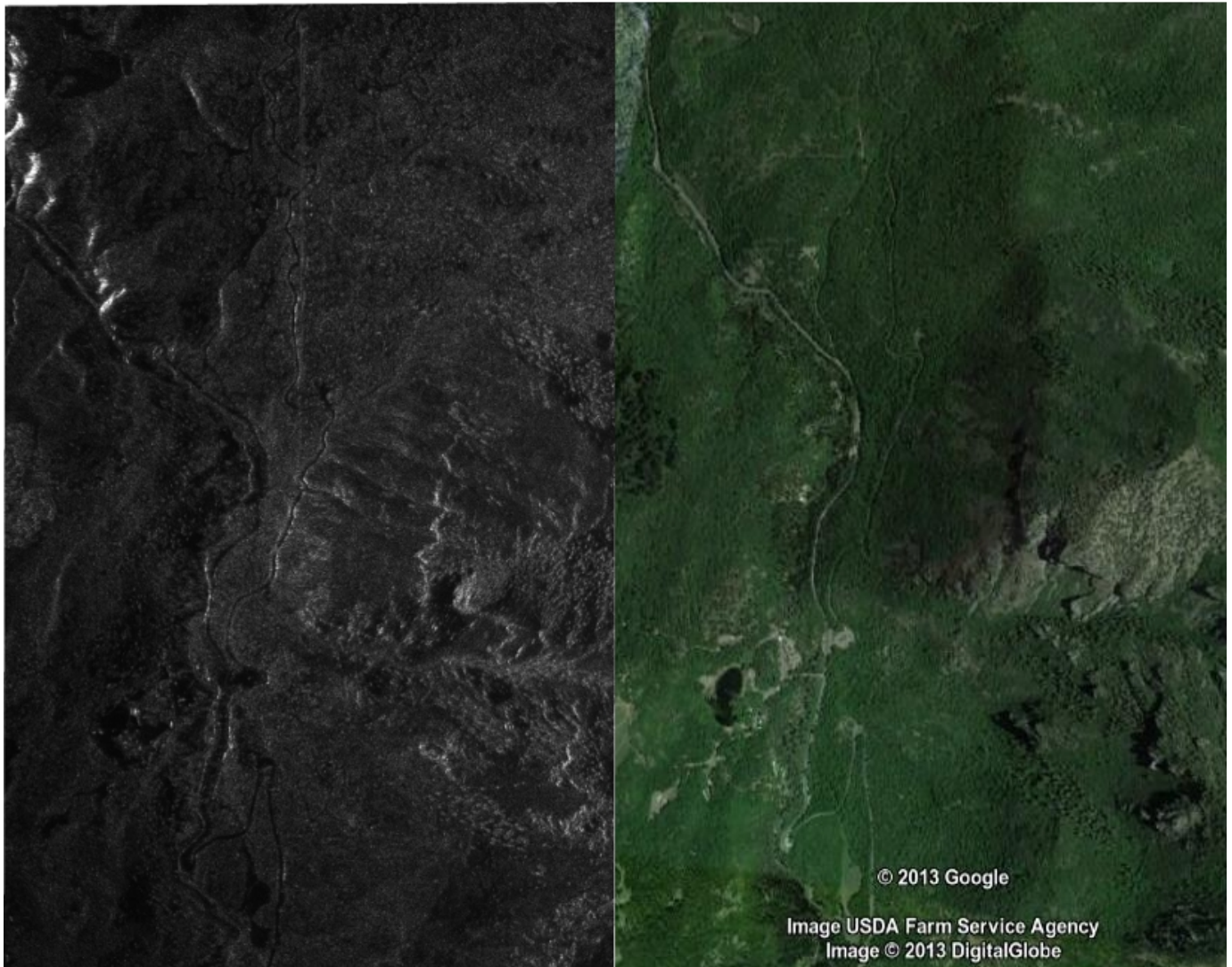
Fig. 8. SAR image of Payson Canyon in Payson, UT compared side-by-side with a corresponding Google Earth image (Courtesy Artemis Inc. and Google Inc.).

and this paper has outlined the fundamental principles that make SAR so versatile.

REFERENCES

[1] M.A. Richards. *Fundamentals of Radar Signal Processing*. McGraw-Hill, New York, NY, 2005.
[2] Fawwaz T. Ulaby, David G. Long, Adrian K. Fung, and Richard K. Moore. *Microwave Remote Sensing Modern Edition*. Artech House, Norwood, MA, 2013.
[3] J.W. Winkler. "An Investigation of Ground Moving Target Indication (GMTI) with a Single-Channel SAR System". Master's thesis, Brigham Young University, 2013.
[4] E.C. Zaugg. "Generalized Image Formation for Pulsed and LFM-CW Synthetic Aperture Radar". Master's thesis, Brigham Young University, 2010.
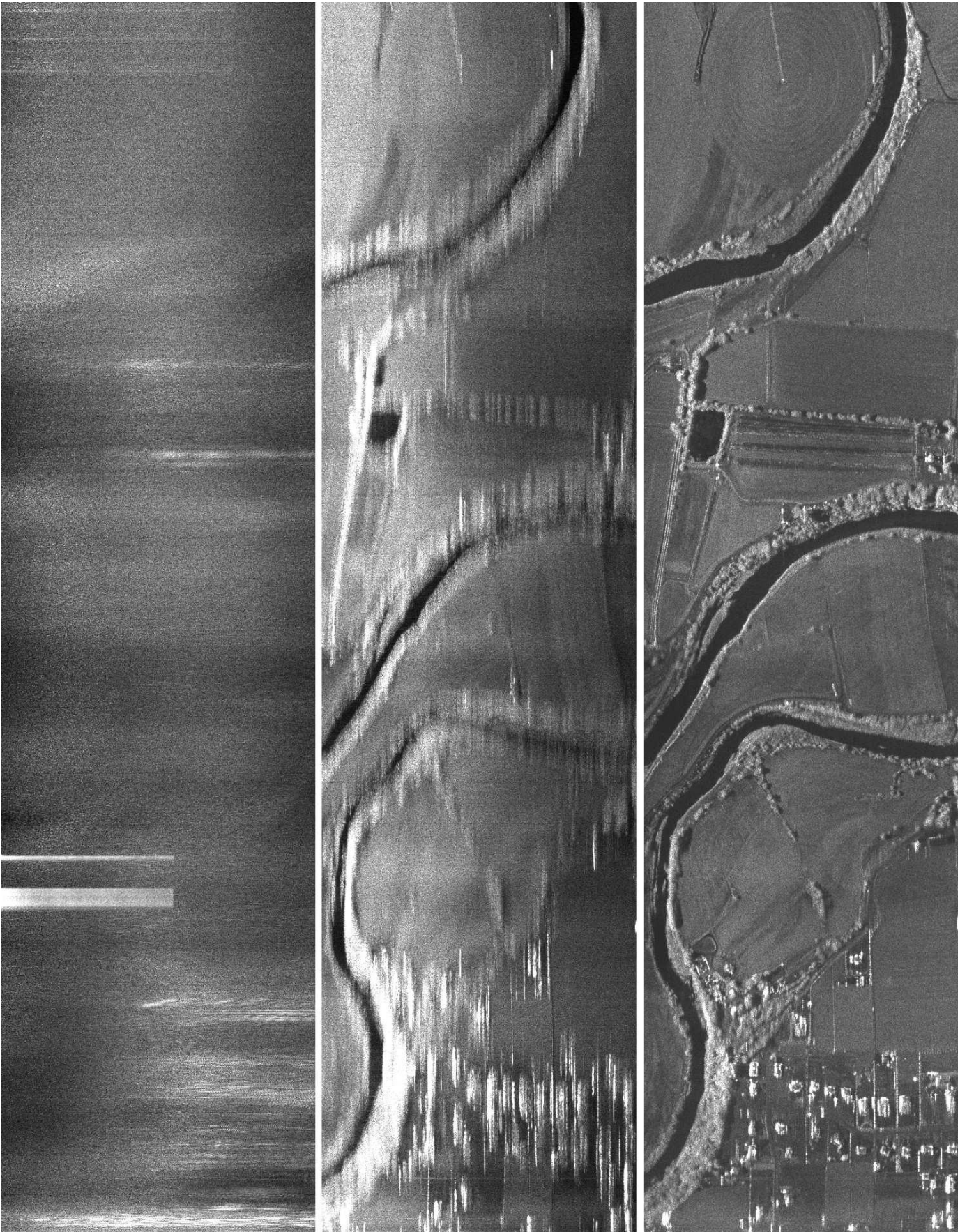
Fig. 9. NuSAR-B X-band data collected over agricultural areas and the Bear River near Elwood and Honeyville, Utah. From left to right the images show the magnitude of the raw data, the magnitude of the range-compressed data, and the magnitude of the azimuth-compressed data, respectively (Courtesy Evan Zaugg, Brigham Young University).